

Neuronal metabolism governs cortical network response state

M. O. Cunningham*, D. D. Pervouchine†, C. Racca*, N. J. Kopell**‡, C. H. Davies§, R. S. G. Jones¶, R. D. Traub||, and M. A. Whittington**‡

*School of Neurology, Neurobiology, and Psychiatry, University of Newcastle, Newcastle upon Tyne NE2 4HH, United Kingdom; †Department of Mathematics, Boston University, 111 Cummington Street, Boston, MA 02215; §Neurology Center of Excellence for Drug Discovery, GlaxoSmithKline, Harlow, Essex CM19 5AW, United Kingdom; ¶Department of Pharmacy and Pharmacology, University of Bath, Bath BA2 7AY, United Kingdom; and ||Department of Physiology and Pharmacology, State University of New York, Brooklyn, NY 11203

Contributed by N. J. Kopell, February 9, 2006

The level of arousal in mammals is correlated with metabolic state and specific patterns of cortical neuronal responsiveness. In particular, rhythmic transitions between periods of high activity (up phases) and low activity (down phases) vary between wakefulness and deep sleep/anesthesia. Current opinion about changes in cortical response state between sleep and wakefulness is split between neuronal network-mediated mechanisms and neuronal metabolism-related mechanisms. Here, we demonstrate that slow oscillations in network state are a consequence of interactions between both mechanisms. Specifically, recurrent networks of excitatory neurons, whose membrane potential is partly governed by ATP-modulated potassium (K_{ATP}) channels, mediate response-state oscillations via the interaction between excitatory network activity involving slow, kainate receptor-mediated events and the resulting activation of ATP-dependent homeostatic mechanisms. These findings suggest that K_{ATP} channels function as an interface between neuronal metabolic state and network responsiveness in mammalian cortex.

glutamate | slow-wave oscillation | potassium channel | rhythm

Slow-wave oscillations (SWO) occur in the cerebral cortex and associated areas (1). They are particularly manifest during periods of behavioral quiescence and are an ubiquitous feature of deep sleep (2–5). Two hypotheses dominate the possible functional significance of such activity (6). SWO have been shown to be critical for learning and plasticity (2, 7). Additionally it has been proposed that they allow for, or are generated by, reduced neuronal metabolism, whereby restorative cellular processes take place to reset the deficit induced by a period of wakefulness (8–10). At the cellular level, slow-wave electroencephalogram activity correlates with fluctuations in the membrane potential of cortical neurones (3, 11), where periods of hyperpolarization (down phase) alternate between periods of depolarization (up phase). Such bistable behavior is thought to depend on a balance of recurrent excitation and local inhibition (12, 13) in addition to slow-wave input from the thalamus (14). However, persistent depolarized states might also occur through synaptic excitation alone, with kinetically slow excitatory synaptic potentials (EPSPs) such as those generated by kainate receptors (15) or NMDA receptors (but see below), temporally summing with sufficient background activity (16). In addition, such a maintained depolarization can be generated purely by intrinsic ionic currents in bistable neurons (17).

The nature of the relationship between neuronal metabolic state and SWO is also unclear. From a network perspective, a number of synaptic conductances, most notably those mediated by NMDA receptors (18), are modulated by metabolism. However, some neurons have intrinsic conductances specifically designed to sense aspects of metabolic state. During wakefulness, constant neuronal activity is metabolically demanding (8, 19). Measurements of cerebral metabolism during slow-wave sleep have demonstrated a decrease in cerebral blood flow in

cortical regions (20) causing restriction of the supply of energy to neuronal populations. One main energy (ATP) consumer is the Na^+/K^+ -ATPase pump, which has been estimated to utilize 50–80% of total cerebral ATP production (8, 19, 21). Therefore, we tested the hypothesis that SWOs depend on interaction between network activity and neuronal metabolism via the metabolism-sensitive intrinsic ionic current gated by intracellular levels of ATP, the K_{ATP} channel (17, 22, 23).

Results

Spontaneous SWO could be recorded in rat entorhinal cortical slices ($n = 62$, 0.17 ± 0.004 Hz) (Fig. 1A). They were seen superficial to lamina dissecans with the largest amplitude occurring in LIII (1018 ± 93.2 μ V). Deeper layers did not show SWO (Fig. 1A). To establish that the SWO were sensitive to the metabolic state of the slice, we modified the glucose concentration used in the bathing medium. Reduction in glucose concentration reduces the ATP/ADP ratio in rat brain (24). The frequency of SWO was higher in 10 mM glucose, as a result of shorter down-phase periods (3.25 ± 0.08 s vs. 4.10 ± 0.3 , $P < 0.05$, $n = 5$) when compared with more physiologically relevant concentrations (25) (2.5 mM, Fig. 1B). The duration of the up phase of the SWO ($P > 0.05$, Fig. 1B) was not altered, suggesting that metabolic state modulated the SWO primarily via effects on the down phase.

Intracellular recordings from layer III pyramidal neurons revealed up and down phases of membrane potential concurrent with the local field potential (Fig. 1C). The two phases were separated by 8.4 ± 0.4 mV ($n = 24$) and demonstrated a clear bistability (Fig. 1Ci). A similar pattern of rhythmic bistability was seen in fast spiking interneurons in LII/III, with membrane potential alternating between phases separated by 7.6 ± 0.6 mV ($n = 5$, Fig. 1Cii). However, stellate cells did not show such a bistable pattern of membrane potential change. Rhythmic increases in spike output, concurrent with the field, were entirely due to trains of fast EPSPs with little temporal summation (Fig. 1Ciii). Layer II neurons are likely to have much less recurrent excitatory connectivity (26) and do not have the large, slow, kainate receptor-mediated postsynaptic responses observed in LIII pyramids** and interneurons (16). We next examined the role of excitatory network activity in the slow oscillation.

Previously, it has been proposed that the generation of the up phase is sensitive to blockade of both NMDA receptors and α -amino-3-hydroxy-5-methyl-4-isoxazolepropionic acid (AMPA)/kainate receptors in neocortex (13). However, in

Conflict of interest statement: No conflicts declared.

Abbreviations: SWO, slow-wave oscillations; AMPA, α -amino-3-hydroxy-5-methyl-4-isoxazolepropionic acid; EPSP, excitatory synaptic potential.

†To whom correspondence may be addressed. E-mail: nk@bu.edu or m.a.whittington@ncl.ac.uk.

**West, P. J. & Wilcox, K. S. (2004) *Soc. Neurosci. Abstr.*, 732.4 (abstr.).

© 2006 by The National Academy of Sciences of the USA

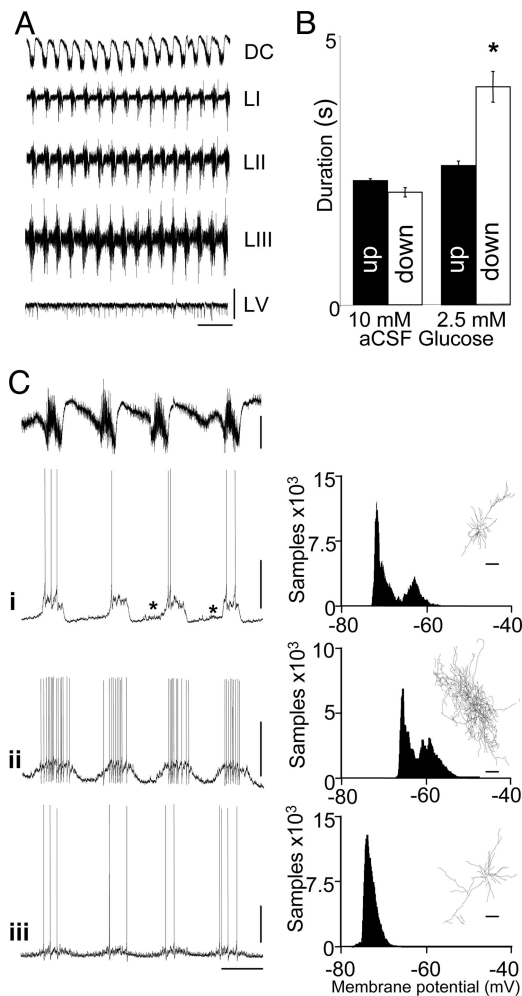


Fig. 1. The profile of SWO in the entorhinal cortex. (A) The example of a DC field potential recording from LIII revealed slow oscillations consisting of alternating periods of activity and quiescence. An array of four extracellular electrodes were placed across the layers of the cortex revealed the anatomical location of the slow rhythm as the superficial entorhinal cortex. Note, no slow rhythm was seen in the deep layer V. (Scale bars, 0.2 mV, 20 s.) (B) The characteristics of the slow rhythm depended on glucose concentration. Switching from 10 mM glucose to 2.5 mM caused a significant prolongation of the down phase (*, $P < 0.05$, $n = 5$). (C) Membrane potential bistability was specific to certain cell types during the slow rhythm. The DC field potential, recorded concurrently with the LIII pyramidal cell data, is shown for reference. (i) LIII pyramidal cells demonstrated the most robust membrane potential bistability. The example trace shows four consecutive transitions from down to up phase (asterisks) also seen in model (Fig. 4E). The histogram shows the distribution of membrane potentials over a 120-s epoch. (Inset) NeuroLucida reconstruction of the recorded neuron. (Scale bars, 50 μ m.) Bistability was also evident in LII basket cells (ii) but not LII stellate cells (iii). (Scale bars, 20 mV, 5 s.)

entorhinal cortex, albeit with a lower calcium ion concentration, we found that the NMDA receptor antagonist D-2-amino-5-phosphonopentanoate (20 mM; $n = 6$) did not block SWO (data not shown). SWO were also unaffected by the AMPA receptor blocker SYM 2206 (25–50 μ M; $n = 6$, Fig. 2A). This not to say that AMPA receptors do not participate in shaping the dynamic of neuronal responses during the up phase, because increases in spike generation in principal cells were evident in the presence of the AMPA receptor blocker (Fig. 2A). Subsequent bath application of the mixed AMPA/kainate receptor antagonist 6-cyano-7-nitroquinoxaline-2,3-dione (CNQX) (20 μ M; $n = 6$) abolished both intracellular and network activity associated with

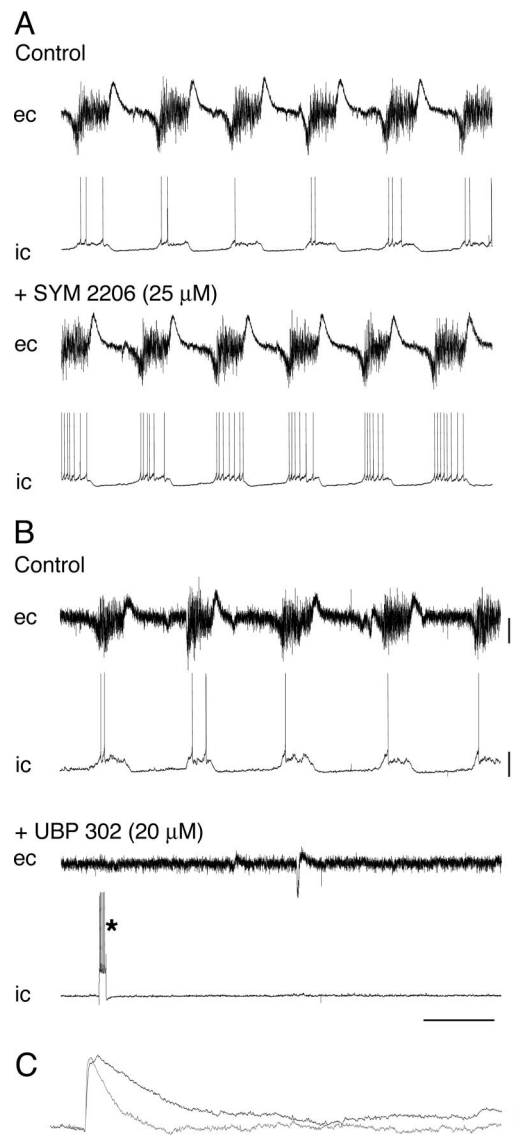


Fig. 2. Kainate receptor activation was critical for generation of the slow oscillation. (A) Concurrent recordings of the LIII field potential and a LIII pyramidal neuron in the absence (Upper) and presence (Lower) of the specific AMPA receptor blocker SYM2206 (25 μ M). There was little change in the slow rhythm in the presence of the drug. Control membrane potential was bistable between -72 ± 2 and -62 ± 3 mV, with sym bistability was between -70 ± 3 and -62 ± 4 mV. (B) In contrast, application of the GluR5 receptor antagonist UBP302 (20 μ M) abolished the rhythmic response-state transitions. At the asterisk, a depolarizing current step demonstrates the continued ability to evoke neuronal responses. Control membrane potential was bistable between -70 ± 1 and -60 ± 1 mV, with UBP302 there was no bistability, membrane potential was monostable around -62 ± 3 mV. [Scale bars, 0.5 mV (field), 20 mV (neuron), 5 s.] (C) Spontaneous excitatory events in LIII pyramids changed dramatically with GluR5 blockade. Data show averaged EPSPs in the presence (gray) and absence (black) of UBP302 (20 μ M). (Scale bars, 0.5 mV, 250 ms.)

the up phase of SWO (data not shown), as seen in neocortex. This finding suggested a role for kainate receptors. Accordingly, bath application of the GluR5-specific receptor antagonist, UBP 302 (20 μ M; $n = 13$), abolished the up phase at both the single-cell and population level (Fig. 2B). In the absence of GluR5-mediated synaptic transmission, spontaneous EPSPs were still recorded, but were considerably briefer than in control (SWO) conditions (Fig. 2C). The decay time constants for

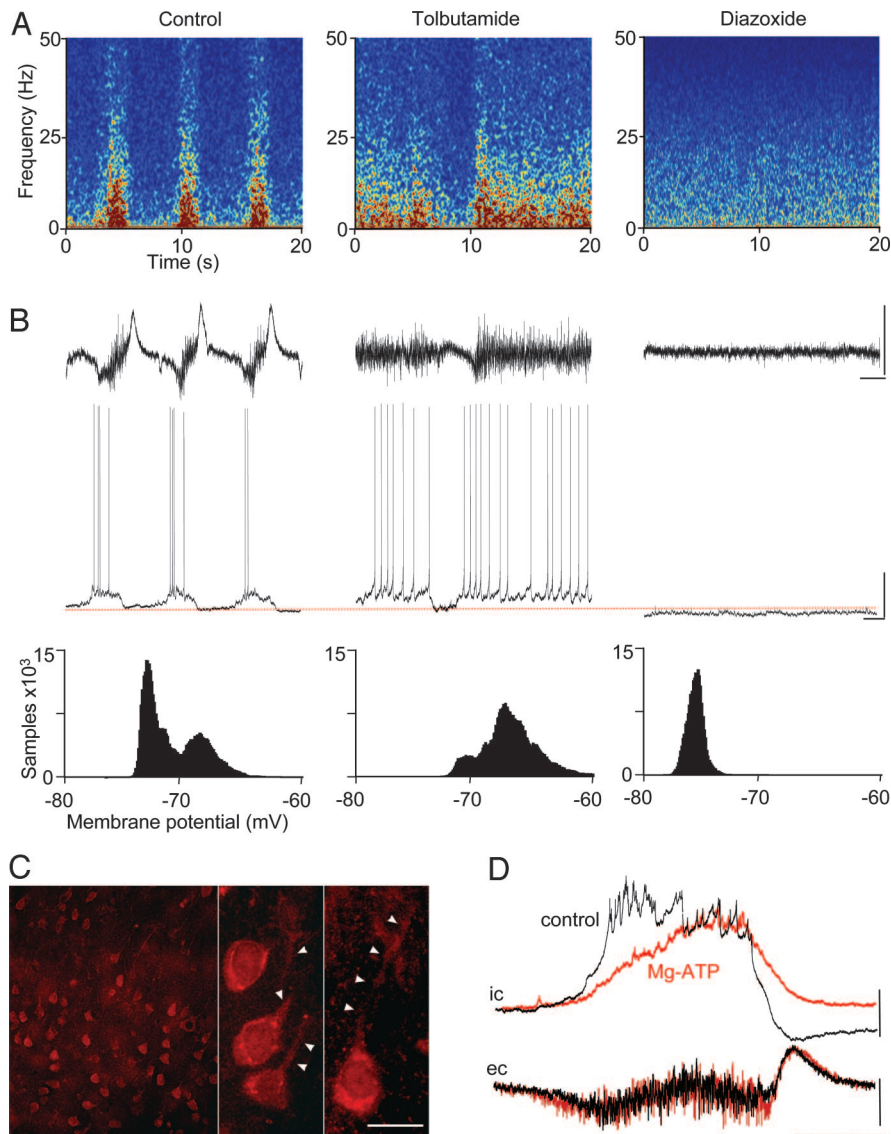


Fig. 3. Rhythmic response-state transitions depend on K_{ATP} channel activity. (A) The LIII extracellular recordings and corresponding spectrograms show the effects of blockade (tolbutamide, 0.5 mM) or activation (diazoxide, 0.3 mM) of K_{ATP} channels on the transition from up to down phases of the oscillation. Each drug was tested on a different set of entorhinal cortex slices. Note the wide spectral content of population activity within the up phase and the prolongation of the up and down phases with K_{ATP} blockade and activation, respectively. [Scale bars, 0.5 mV (field), 1 s.] Longer epochs of data, with drug wash-out examples, are illustrated in Fig. 6, which is published as supporting information on the PNAS web site. (B) Intracellular recordings from LIII pyramidal neurons taken concurrently with the data shown in A. Action potentials are truncated to display the predominant membrane potential during the disrupted slow oscillation. Each recording was taken 10–20 min after impalement in each of the three experimental conditions. The red line indicates the resting membrane potential (–75 mV). Shown below are the corresponding membrane potential histograms demonstrating disrupted bistability when K_{ATP} channels are exogenously activated or blocked. [Scale bars, 20 mV, 1 s.] (C) Distribution of Kir6.2 immunoreactive cells in layer III (Left). (Center and Right) Examples of layer III pyramidal cells positive for Kir6.2. Arrowheads point to labeled dendrites. (Scale bar, 30 μ m in Left and 20 μ m in Center and Right.) (D) Membrane potential triggered averages of 10 consecutive periods of slow oscillation (ic) in a LIII pyramid in control conditions (black) and in a pyramid recorded with an electrode filled with 50 mM MgATP (red) to block K_{ATP} channels only in the recorded cell ($n = 5$ cells). Note the absence of a post-up-phase hyperpolarization with MgATP and a slowed transition to peak up phase. (Scale bars, 5 mV, 1 s.) Corresponding averages ($n = 10$ periods) of field data (LIII, ec) show no change in population activity when K_{ATP} channels are blocked in a single neuron. (Scale bars, 0.2 mV, 1 s.)

spontaneous EPSPs recorded in layer III pyramidal neurons decreased from 109 ± 5 ms to 14 ± 1 ms ($P < 0.05$, $n = 5$). These data suggested that, as with interneurons (16), temporal summation of kainate receptor-mediated recurrent excitatory activity within a LIII pyramidal neuronal network played a role in the generation and maintenance of the up phase of the SWO.

The above data support the notion that the up phase was driven by recurrent network excitation but that the metabolic sensitivity of the SWO is mediated by effects on the down phase. Therefore, we examined the mechanisms underlying the transi-

tion between two phases of the SWO cycle. In addition to network dynamics, the intrinsic properties of neurons play a fundamental role in governing cortical bistable activity (27). One possibility is that a K^+ current activated by the metabolic demands ($[ATP]:[ADP]$) of network activity during the up phase of the oscillation may drive the transition to down phase. We tested the involvement of K_{ATP} channels pharmacologically. Antagonism with tolbutamide (300 μ M; $n = 6$), caused a significant prolongation of the up phase (control vs. tolbutamide: 2.92 ± 0.04 s vs. 9.21 ± 0.76 s; $P < 0.001$; Fig. 3 A and B) and

activation with diazoxide (300–500 μM ; $n = 6$) increased the duration of the down phase at both neuron and network level (control vs. diazoxide: 5.08 ± 0.82 s vs. 11.71 ± 1.89 s; $P < 0.001$; Fig. 3A and B). Immunocytochemical experiments where slices were stained for one of the pore forming subunits, Kir6.2, confirmed the presence of the K_{ATP} channel in the LIII neurons involved in the SWO (Fig. 3C).

The relative contribution of synaptic network properties and K_{ATP} channels in SWO was examined by blocking the channels only in a single recorded neuron by addition of 50 mM MgATP to the intracellular recording solution (28). Blockade of K_{ATP} in a single LIII pyramidal neuron did not affect the population oscillation. However, the transition from down to up phase in the recorded neuron ($n = 5$) was prolonged, and the post-up-phase hyperpolarization was abolished (Fig. 3D). In these cells the residual waveform (Fig. 3D, red trace) can be regarded as the average synaptic input to the cell in the absence of the intrinsic waveform generated by interplay between this network activity and K_{ATP} channels. These data suggested that both the individual cellular response to network activity and the termination of the up phase were governed by modulation of K_{ATP} channels, most likely formed by Kir6.2-SUR1 (29).

These data indicate that interactions between kainate receptor-mediated activity in a recurrent network of pyramidal neurons and the metabolic demands of these neurons (expressed via modulation of K_{ATP} channels) was sufficient to generate rhythmic population bistability. Given the degree of action potential generation associated with the up phase of the SWO the most likely candidate mechanism for coupling activity to the K_{ATP} channels was ATP utilization by the Na^+/K^+ pump. Ouabain (0.5 mM), which blocks $\text{Na}^+/\text{K}^+-\text{ATPase}$ (30), abolished the SWO (data not shown). Changes in extracellular calcium ion concentration also occur during SWO (31). Both synaptic activity and spiking are associated with increased calcium entry into neurons, which are pumped out by a $\text{Ca}^{2+}-\text{ATPase}$ (32). However, for the present model, we consider the effects of spike-induced changes in $[\text{Na}^+]_i$ only. We constructed a model in which recurrent network activity in excitatory neurons interacted with K_{ATP} channels in a manner dependent on ATP hydrolysis (via $\text{Na}^+/\text{K}^+-\text{ATPase}$) in response to action potential-dependent $[\text{Na}^+]_i$ increases.

Starting with random initial conditions, the model population of 100 cells produced SWO with 10–11 active periods per min (Fig. 4A). The up phase consisted of temporally summed EPSPs. As long as τ_d was >16 ms, below this value, no SWO was seen. Spiking caused increases in $[\text{Na}^+]_i$ in each cell (Fig. 4B), thus decreasing $[\text{ATP}]_i$ (Fig. 4C) leading to the opening of the K_{ATP} channels (Fig. 4D), which generated a membrane hyperpolarization. However, because of the recurrent excitatory synaptic connections, cell spiking continued until a threshold was reached at which synaptic drive could no longer sustain the population activity, the termination of the up phase.

During the down phase, ATP levels recovered, gradually removing the influence of K_{ATP} on membrane potential. The resulting gradual depolarization increased background activity within the recurrent network (Fig. 4E) until, again, a threshold is reached. Positive feedback between the increase in recurrent excitation and the membrane potential effectively bootstraps the network back into the up phase via temporal summation of EPSPs. With a heterogeneous bias current across the population of neurons, the onset of the up phase is triggered by the mutual recruitment of subpopulations of the most active neurons, which act to excite the rest of the population. This model was able to reproduce the effects of experimental manipulation of K_{ATP} channels with tolbutamide and diazoxide (compare Fig. 3A and B with Fig. 5, which is published as supporting information on the PNAS web site).

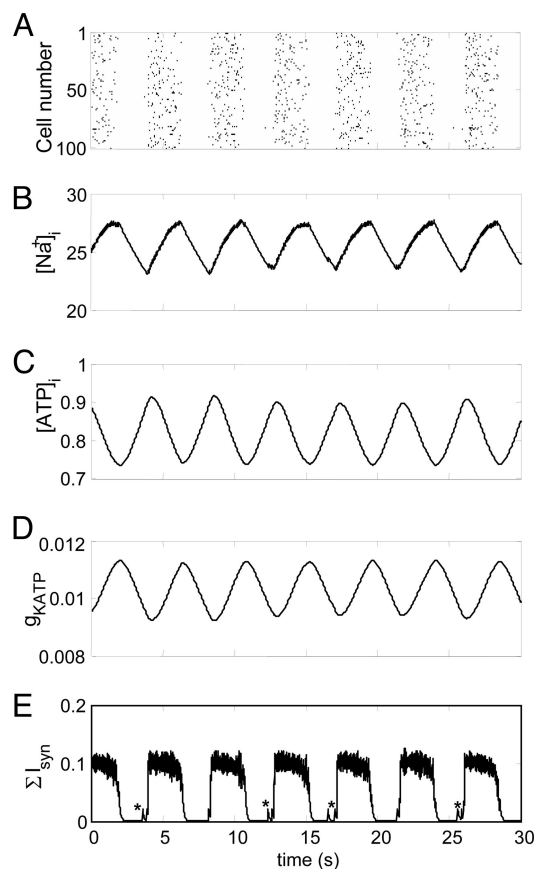


Fig. 4. Computational model predicts network bistability generated by interactions between recurrent excitatory network and K_{ATP} channel activity alone. (A) Raster plot of spiking in a network of 100 neurons showing slow rhythmic transitions between up and down phases synchronously throughout the network. Each neuron was coupled into an excitatory network by EPSPs with decay time constant of 100 ms, and each neuron had g_{KATP} . Each dot corresponds to one action potential. (B) Concurrent plot of $[\text{Na}^+]_i$ showing gradual elevation in intracellular sodium ion concentration during the up phase of the rhythm. (C) As $[\text{Na}^+]_i$ increases $[\text{ATP}]_i$ falls as the neurons attempt to restore electrochemical equilibrium via $\text{Na}^+/\text{K}^+-\text{ATPase}$ activity. Note changes in $[\text{Na}^+]_i$ and $[\text{ATP}]_i$ are in antiphase. (D) The dynamics of $[\text{ATP}]_i$ lead to a concurrent modulation in g_{KATP} , which peaks on transition from the up to down phase. This, coupled with the resulting modulation of recurrent network activity (shown here as the total excitatory synaptic input current to one neuron, ΣI_{syn} E), leads to a temporal pattern of membrane potential change associated with the slow rhythm in entorhinal cortical LIII pyramids. Note the model also reproduces the increase in background EPSP generation before transition to up phase also seen in experiment (asterisks, see Fig. 1C). Further examples of the model's behavior with manipulation of g_{KATP} are illustrated in Fig. 5.

SWOs recorded *in vitro* brain slice preparations very closely resemble those seen *in vivo* (data in this study and also compare data in refs. 2–5 and 11 with data in refs. 12 and 13). Even in the absence of a thalamic SWO generator (14), the present computational and experimental data indicated that rhythmic bistability in cortical neuronal networks can occur as a consequence of the thresholding effects of the interaction between neurons coupled via kainate receptor-mediated excitation and the resulting metabolic demands influencing membrane potential via K_{ATP} channels. The possibility of generation of an active up phase in neurons generated by temporal summation of kainate receptor-mediated postsynaptic events (16) suggests that recurrent excitatory networks, so coupled, may serve to control intrinsic network responsivity on the basis of brain metabolic state. In the present study, kainate receptors alone were neces-

sary and sufficient to generate this network bistability. However, AMPA receptors played a role in shaping the faster dynamics of the system within an up phase. Interneurons in cortex receive a large part of their synaptic drive via these receptors, suggesting that the increase in principal cell spiking during the up phase in the absence of AMPA receptor-mediated synaptic transmission (Fig. 2*A*) occurred via disinhibition.

The role of ATP in neuronal metabolism may strongly influence neuronal information processing (33). The present data indicate that, given the interaction between ATP and potassium channels and the relationship between sleep and neuronal metabolism (6, 9), the state of cortical arousal may be controlled primarily by the activity of such networks.

Methods

Electrophysiology. Horizontal entorhinal cortical slices (450 μm thick) were prepared from adult male Wistar rats (150–250 g) and maintained at 34°C at the interface between warm moist carbogen gas (95% O_2 /5% CO_2) and artificial cerebrospinal fluid (aCSF) containing 3 mM KCl, 1.25 mM NaH_2PO_4 , 1 mM MgSO_4 , 1.6 mM CaCl_2 , 24 mM NaHCO_3 , 10 or 2.5 mM glucose, and 126 mM NaCl. Field recordings were made by using glass micropipettes filled with aCSF (resistance 0.5–2 M Ω) either as DC or high-pass filtered at 0.1 Hz. Intracellular recordings were made by using pipettes filled with 2 M potassium methylsulphate (resistance, 60–90 M Ω). Recorded neurons were filled with biocytin for identification and post hoc reconstruction.

Immunocytochemistry. Sections of entorhinal cortex were sandwiched between two Millipore filters to prevent deformations,

fixed for 1–7 days in 4% paraformaldehyde in 0.1 M PBS (pH 7.4), and then gelatin-embedded. All tissue was sectioned at 60- μm thickness and processed for fluorescence light microscopy immunocytochemistry as described in Racca *et al.* (34). Briefly, a sheep (kind gift of Asipu Sivaprasadarao, University of Leeds, Leeds, U.K.) or rabbit (Alomone Labs, Jerusalem) anti-Kir6.2 antibody (1:100) was visualized with Cy3-conjugated donkey anti-sheep or -rabbit antibody (1:500; Jackson ImmunoResearch). Sections were mounted on glass slides and coverslipped with Vectashield (Vector Laboratories) before being examined with a standard fluorescence light microscope (Zeiss).

Modeling. Layer III pyramidal cells are modeled by using standard single-compartment Hodgkin–Huxley formalism (fast Na^+ current, delayed-rectifier K^+ current, leak currents), an extra after-hyperpolarization current, stochastic persistent Na^+ current, and ATP-sensitive K^+ current. The dynamic equations are summarized in *Appendix*, which is published as supporting information on the PNAS web site. In addition, each cell contains two extra variables, the concentration of ATP and the intracellular concentration of Na^+ . The population of $n = 100$ such cells is randomly connected (each cell receives input from 10% of the population) using weak “kainate” synapses (raise time, 0.5 ms; decay time, 100 ms). Detailed modeling methods and parameters are given in *Appendix*.

We thank Stuart Greenhill for assistance with experiments involving UBP302. This work was supported by The Medical Research Council (U.K.), The National Institutes of Health, GlaxoSmithKline Plc, and The Wellcome Trust.

- Wilson, C. J. & Groves, P. M. (1981) *Brain Res.* **220**, 67–80.
- Steriade, M. (2003) *Neuronal Substrates of Sleep and Epilepsy* (Cambridge Univ. Press, Cambridge, U.K.).
- Steriade, M., Nuñez, A. & Amzica, F. (1993) *J. Neurosci.* **13**, 3252–3265.
- Contreras, D. & Steriade, M. (1995) *J. Neurosci.* **15**, 604–622.
- Contreras, D., Timofeev, I. & Steriade, M. (1996) *J. Physiol. (London)* **494**, 251–264.
- Hairston, I. S. & Knight, R. T. (2004) *Nature* **430**, 27–28.
- Lee, A. K. & Wilson, M. A. (2002) *Neuron* **36**, 1183–1194.
- Ames, A., III (2000) *Brain Res. Brain Res. Rev.* **34**, 42–68.
- Maquet, P. (1995) *Behav. Brain Res.* **69**, 75–83.
- Porkka-Heiskanen, T., Strecker, R. E., Thakkar, M., Bjorkum, A. A., Greene, R. W. & McCarley, R. W. (1997) *Science* **276**, 1265–1268.
- Steriade, M., Nuñez, A. & Amzica, F. (1993) *J. Neurosci.* **13**, 3266–3283.
- Shu, Y., Hasenstaub, A. & McCormick, D. A. (2003) *Nature* **423**, 288–293.
- Sanchez-Vives, M. V. & McCormick, D. A. (2000) *Nat. Neurosci.* **3**, 1027–1034.
- Hughes, S. W., Cope, D. W., Blethyn, K. L. & Crunelli, V. (2002) *Neuron* **33**, 947–958.
- Castillo, P. E., Malenka, R. C. & Nicoll, R. A. (1997) *Nature* **388**, 182–186.
- Frerking, M. & Ohliger-Frerking, P. (2002) *J. Neurosci.* **22**, 7434–7443.
- Cook, D. L. & Hales, C. N. (1984) *Nature* **311**, 271–273.
- Aizenman, E., Lipton, S. A. & Loring, R. H. (1989) *Neuron* **2**, 1257–1263.
- Attwell, D. & Laughlin, S. B. (2001) *J. Cereb. Blood Flow Metab.* **21**, 1133–1145.
- Zoccoli, G., Walker, A. M., Lenzi, P. & Franzini, C. (2002) *Sleep Med. Rev.* **6**, 443–455.
- Erecinska, M. & Silver, I. A. (1989) *J. Cereb. Blood Flow. Metab.* **9**, 2–19.
- Ashcroft, S. J. & Ashcroft, F. M. (1990) *Cell Signal.* **2**, 197–214.
- Ashcroft, F. M. & Gribble, F. M. (1998) *Trends Neurosci.* **21**, 288–294.
- Ekholm, A., Katsura, K., Kristian, T., Liu, M., Folbergeova, J. & Siesjo, B. K. (1993) *Brain Res.* **604**, 185–191.
- Silver, I. A. & Erecinska, M. (1994) *J. Neurosci.* **14**, 5068–5076.
- Dhillon, A. & Jones, R. S. G. (2000) *Neuroscience* **99**, 413–422.
- Loewenstein, Y., Mahon, S., Chadderton, P., Kitamura, K., Sompolinsky H., Yarom, Y. & Hausser, M. (2005) *Nat. Neurosci.* **8**, 202–211.
- Jiang, C. & Haddad, G. G. (1997) *J. Neurophysiol.* **77**, 93–102.
- Gribble, F. M., Ashfield, R., Ammala, C. & Ashcroft, F. M. (1997) *J. Physiol. (London)* **498**, 87–98.
- Thomas, R. C. (1969) *J. Physiol. (London)* **201**, 495–514.
- Massimi, M. & Amzica, F. (2001) *J. Neurophysiol.* **85**, 1346–1350.
- Gill, D. L., Chueh, S. H. & Whitlow, C. L. (1984) *J. Biol. Chem.* **259**, 10807–10813.
- Laughlin, S. B., de Ruyter van Steveninck, R. R. & Anderson, J. C. (1998) *Nat. Neurosci.* **1**, 36–41.
- Racca, C. (1997) *J. Neurosci.* **77**, 1691–1700.